

## Band Structure Asymmetry of Bilayer Graphene Revealed by Infrared Spectroscopy

Z. Q. Li,<sup>1,\*</sup> E. A. Henriksen,<sup>2</sup> Z. Jiang,<sup>2,3</sup> Z. Hao,<sup>4</sup> M. C. Martin,<sup>4</sup> P. Kim,<sup>2</sup> H. L. Stormer,<sup>2,5,6</sup> and D. N. Basov<sup>1</sup>

<sup>1</sup>*Department of Physics, University of California, San Diego, La Jolla, California 92093, USA*

<sup>2</sup>*Department of Physics, Columbia University, New York, New York 10027, USA*

<sup>3</sup>*National High Magnetic Field Laboratory, Tallahassee, Florida 32310, USA*

<sup>4</sup>*Advanced Light Source Division, Lawrence Berkeley National Laboratory, Berkeley, California 94720, USA*

<sup>5</sup>*Department of Applied Physics and Applied Mathematics, Columbia University, New York, New York 10027, USA*

<sup>6</sup>*Bell Labs, Alcatel-Lucent, Murray Hill, New Jersey 07974, USA*

(Received 11 July 2008; published 23 January 2009)

We report on infrared spectroscopy of bilayer graphene integrated in gated structures. We observe a significant asymmetry in the optical conductivity upon electrostatic doping of electrons and holes. We show that this finding arises from a marked asymmetry between the valence and conduction bands, which is mainly due to the inequivalence of the two sublattices within the graphene layer and the next-nearest-neighbor interlayer coupling. From the conductivity data, the energy difference of the two sublattices and the interlayer coupling energy are directly determined.

DOI: 10.1103/PhysRevLett.102.037403

PACS numbers: 78.30.Na, 73.63.-b, 78.66.Tr, 78.67.-n

Recently there has been unprecedented interest in carbon-based materials due to the discovery of graphene [1]. Among all carbon systems, bilayer graphene stands out due to its remarkable properties such as a unique quantum Hall effect stemming from a previously unknown type of quasiparticles, massive chiral quasiparticles [2]. Bilayer graphene is predicted to show strong many body interactions due to the unusual shape of the Fermi surface [3]. Moreover, it is the only known semiconductor with a tunable band gap between the valence and conduction bands [4–7], which demonstrates its great potential for future nanoelectronic applications. Therefore, it is of utmost importance to acquire a comprehensive understanding of this material. One central issue is how the Dirac quasiparticles in single layer graphene are modified when two graphene sheets are stacked together in bilayer graphene. The vast majority of previous experimental and theoretical studies have assumed that the electronic band structure of bilayer graphene is symmetric. This is in contrast with a significant electron-hole asymmetry observed in cyclotron resonance [8] and cyclotron mass experiments [4]. Several theoretical proposals have been put forward to explain these results [4,9]. However, our current understanding of the observed effects remains incomplete. Furthermore, the interlayer coupling energy  $\gamma_1$  that controls the fundamental properties of bilayer graphene is yet to be determined [4,10,11].

Here we present the first investigation of the optical conductivity of bilayer graphene via infrared spectroscopy. We observed dramatic differences in the evolution of the conductivity for electron and hole polarities of the gate voltage. We show that small band parameters other than  $\gamma_1$  give rise to an asymmetry between the valence and conduction bands [10], in contrast to the commonly assumed symmetric band structure. The systematic character of our IR data enables us to extract an energy difference between the *A* and *B* sublattices within the same graphene

layer [Fig. 1(b)] of  $\Delta' \approx 18$  meV. Moreover, the value of  $\gamma_1$ ,  $\approx 404$  meV, is determined from direct measurements of interband transitions. We discuss the broad implications of these findings for the fundamental understanding of bilayer graphene.

Infrared reflectance  $R(\omega)$  and transmission  $T(\omega)$  measurements were performed on bilayer graphene samples on SiO<sub>2</sub>/Si substrate [8] as a function of gate voltage  $V_g$  at 45 K employing synchrotron radiation, as described in [12]. We find that both  $R(\omega)$  [13,14] and  $T(\omega)$  spectra of the bilayer graphene device can be strongly modified by a gate voltage. Figure 1 shows the transmission ratio data at several voltages normalized by data at the charge neutrality voltage  $V_{CN}$ :  $T(V)/T(V_{CN})$ , where  $V_{CN}$  is the voltage corresponding to the minimum dc conductivity, and  $V = V_g - V_{CN}$ . The  $T(V)/T(V_{CN})$  spectra are dominated by a dip at around 3000 cm<sup>-1</sup>, the magnitude of which increases systematically with voltage. Apart from the main dip, a peak was observed in the  $T(V)/T(V_{CN})$  data below 2500 cm<sup>-1</sup>, which shifts systematically with voltage. This latter feature is similar to the  $T(V)/T(V_{CN})$  data for single layer graphene [12]. The gate-induced enhancement in transmission [ $T(V)/T(V_{CN}) > 1$ ] below 2500 cm<sup>-1</sup> and above 3500 cm<sup>-1</sup> implies a decrease of the absorption with voltage in these frequency ranges.

The most informative quantity for exploring the quasiparticle dynamics in bilayer graphene is the two-dimensional optical conductivity  $\sigma_1(\omega) + i\sigma_2(\omega)$  [12,15]. First, we extracted the optical conductivity at  $V_{CN}$  from the reflectance data (not shown) employing a multilayer analysis of the device [12,15]. We find that  $\sigma_1(\omega, V_{CN})$  has a value of  $2(\pi e^2/2h)$  at high energies, with a pronounced peak at 3250 cm<sup>-1</sup> [inset of Fig. 2(b)]. This observation is in agreement with theoretical analysis on undoped bilayer graphene [16–18]. Our high energy data agree with recent experiments in the visible region [19]. The peak around

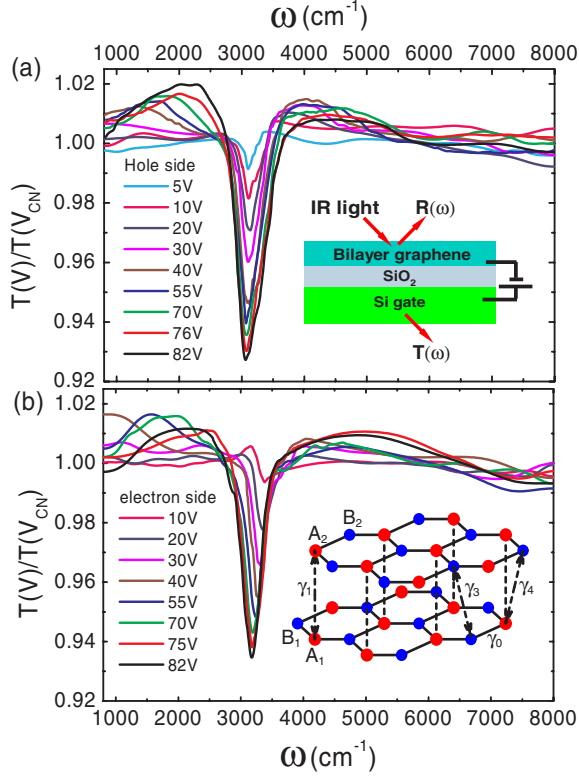


FIG. 1 (color online).  $T(V)/T(V_{CN})$  spectra of bilayer graphene. (a),(b) Data for  $E_F$  on the hole side and electron side. Inset of (a): A schematic of the device and infrared measurements. Inset of (b): A schematic of bilayer graphene with the interlayer coupling parameters shown. The  $A$  and  $B$  sublattices are shown in different colors. The sublattice  $A_2$  is right on top of the sublattice  $A_1$ .

$3250 \text{ cm}^{-1}$  can be assigned to the interband transition in undoped bilayer near the interlayer coupling energy  $\gamma_1$ .

An applied gate voltage shifts the Fermi energy  $E_F$  to finite values leading to significant modifications of the optical conductivity. The  $\sigma_1(\omega, V)$  and  $\sigma_2(\omega, V)$  spectra extracted from voltage-dependent reflectance and transmission data [12] are shown in Fig. 2. At frequencies below  $2500 \text{ cm}^{-1}$ , we observe a suppression of  $\sigma_1(\omega, V)$  below  $2(\pi e^2/2h)$  and a well-defined threshold structure, the energy of which systematically increases with voltage. Significant conductivity was observed at frequencies below the threshold feature. These observations are similar to the data in single layer graphene [12]. The threshold feature below  $2500 \text{ cm}^{-1}$  can be attributed to the onset of interband transitions at  $2E_F$ , as shown by the arrow labeled  $e_1$  in the insets of Figs. 2(a) and 2(b). The observed residual conductivity below  $2E_F$  is in contrast to the theoretical absorption for ideal bilayer graphene [17,18] that shows nearly zero conductivity up to  $2E_F$ . Similar to single layer graphene, the residual conductivity may originate from disorder effects [17] or many body interactions [12]. Apart from the above similarities, the optical conductivity of bilayer graphene is significantly different from the single layer conductivity. First, the energy range where

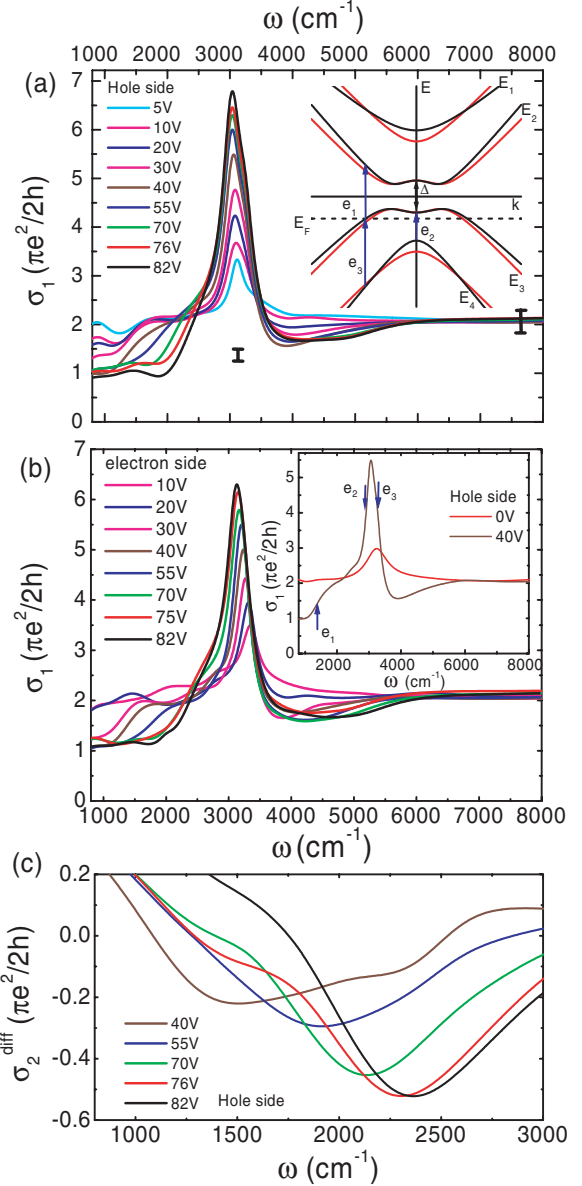


FIG. 2 (color online). The optical conductivity of bilayer graphene. (a),(b)  $\sigma_1(\omega, V)$  data for  $E_F$  on the hole side and electron side. (c)  $\sigma_2^{\text{diff}}(\omega, V)$  spectra in the low frequency range, after subtracting the Lorentzian oscillators describing the main resonance around  $3000 \text{ cm}^{-1}$  from the whole  $\sigma_2(\omega, V)$  spectra. Inset of (a): Schematics of the band structure of bilayer with zero values of  $\Delta'$  and  $v_4$  [gray curve (red)] and finite values of  $\Delta'$  and  $v_4$  (black curve), together with allowed interband transitions. Inset of (b):  $\sigma_1(\omega, V)$  at  $0 \text{ V}$  ( $V_{CN}$ ) and  $40 \text{ V}$  on the hole side with assignments of the features.

the conductivity  $\sigma_1(\omega, V)$  is impacted by the gate voltage extends well beyond the  $2E_F$  threshold. Furthermore, we find a pronounced peak near  $3000 \text{ cm}^{-1}$ , the oscillator strength of which shows a strong voltage dependence. This peak originates from the interband transition between the two conduction bands or two valence bands [inset of Fig. 2(a)] [17,18].

The Fermi energy of bilayer graphene can be extracted from  $\sigma_2(\omega, V)$  [12]. In order to isolate the  $2E_F$  feature, we fit the main resonance near  $3000 \text{ cm}^{-1}$  with Lorentzian oscillators and then subtracted them from the experimental  $\sigma_2(\omega, V)$  spectra to obtain  $\sigma_2^{\text{diff}}(\omega, V)$ . The latter spectra reveal a sharp minimum at  $\omega = 2E_F$  [Fig. 2(c)] similar to monolayer graphene [12]. Figure 3(a) depicts the experimental  $2E_F$  values along with the theoretical result in [7]. Our data can be fitted assuming the Fermi velocity and interlayer coupling in the following parameter space:  $v_F = 1.0\text{--}1.1 \times 10^6 \text{ m/s}$  and  $\gamma_1 = 360\text{--}450 \text{ meV}$ . As shown in [7], the band gap  $\Delta_{\text{gap}}(V)$  is much smaller than  $2E_F(V)$ , and therefore has negligible effects on the experimentally observed  $2E_F(V)$  behavior.

The central result of our study is an observation of a pronounced asymmetry in evolution of the optical conductivity upon injection of electrons or holes in bilayer graphene. Specifically, the frequencies of the main peak  $\omega_{\text{peak}}$  in  $\sigma_1(\omega, V)$  are very distinct for  $E_F$  on the electron and hole sides, as shown in Fig. 3(b). In addition,  $\omega_{\text{peak}}$  on the electron side shows a much stronger voltage dependence compared to that on the hole side. All these features are

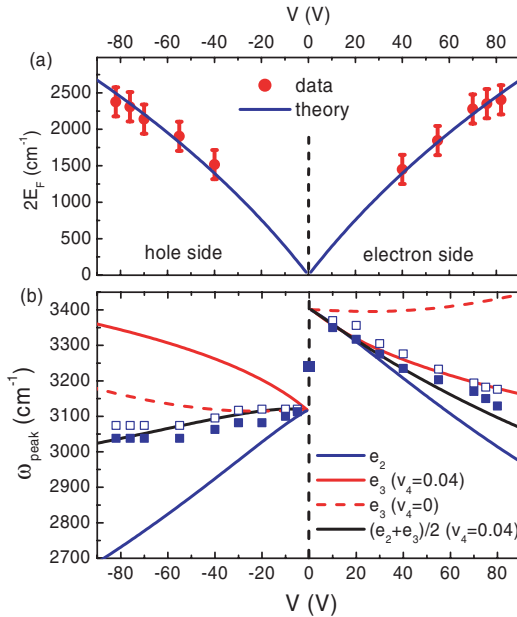


FIG. 3 (color online). (a) Symbols: The  $2E_F$  values extracted from the optical conductivity detailed in the text. The error bars are estimates of the uncertainties of  $\sigma_2^{\text{diff}}(\omega, V)$  spectra in Fig. 2(c). Solid lines: The theoretical  $2E_F$  values using  $v_F = 1.1 \times 10^6 \text{ m/s}$  and  $\gamma_1 = 450 \text{ meV}$ . (b) Solid symbols: The energy of the main peak  $\omega_{\text{peak}}$  in the  $\sigma_1(\omega, V)$  spectrum. Open symbols: The energy of the dip feature  $\omega_{\text{dip}}$  in the  $T(V)/T(V_{CN})$  spectra. Note that  $\omega_{\text{peak}}$  in  $\sigma_1(\omega, V)$  is shifted from  $\omega_{\text{dip}}$  in the raw  $T(V)/T(V_{CN})$  data with an almost constant offset, which is due to the presence of the substrate. Solid lines: Theoretical values of the transitions at  $e_2$ ,  $e_3$ , and  $(e_2 + e_3)/2$  with  $v_F = 1.1 \times 10^6 \text{ m/s}$ ,  $\gamma_1 = 404 \text{ meV}$ ,  $\Delta' = 18 \text{ meV}$ , and  $v_4 = 0.04$ . Red dashed lines:  $e_3$  with similar parameters except  $v_4 = 0$ .

evident in the raw data in Fig. 1, where the resonance leads to a dip in  $T(V)/T(V_{CN})$  spectra. These behaviors are reproducible in multiple gated samples. Such an electron-hole asymmetry is beyond a simple band structure only taking  $\gamma_1$  into account, which predicts symmetric properties between electron and hole sides.

The electron-hole asymmetry in our  $\sigma_1(\omega, V)$  data can be explained by an asymmetry between valence and conduction bands [20]. Such an asymmetric band structure arises from finite band parameters  $\Delta'$  and  $v_4$ , where  $\Delta'$  (denoted as  $\Delta$  in [17,21]) is the energy difference between  $A$  and  $B$  sublattices within the same graphene layer, and  $v_4 = \gamma_4/\gamma_0$ .  $\gamma_4$  and  $\gamma_0$  are defined as interlayer next-nearest-neighbor coupling energy and in-plane nearest-neighbor coupling energy, respectively [17,21]. We first illustrate the effects of  $\Delta'$  and  $v_4$  on the energy bands of bilayer graphene  $E_i(k)$  ( $i = 1, 2, 3, 4$ ), which can be obtained from solving the tight binding Hamiltonian Eq. 6 in Ref. [17]. It is evident that finite values of  $\Delta'$  and  $v_4$  break the symmetry between valence and conduction bands, as schematically shown in the inset of Fig. 2(a). Specifically,  $\Delta'$  induces an asymmetry in  $E_1$  and  $E_4$  bands such that  $E_1 > -E_4$  at  $k = 0$ , whereas  $v_4$  induces an electron-hole asymmetry in the slope of the valence and conduction bands. With finite  $v_4$ , the bands  $E_1$  and  $E_2$  are closer and  $E_3$  and  $E_4$  are further apart at high  $k$  compared to those with zero  $v_4$  value.

Next we examine the effects of  $\Delta'$  and  $v_4$  on  $\sigma_1(\omega, V)$ . It was predicted theoretically [18] that the main peak in  $\sigma_1(\omega, V)$  occurs in the frequency range between two transitions labeled  $e_2$  and  $e_3$  as shown in the insets of Figs. 2(a) and 2(b). Here  $e_2 = -E_4(k=0) - \Delta_{\text{gap}}/2$  and  $e_3 = E_3(k=k_F) - E_4(k=k_F)$  for the hole side, and  $e_2 = E_1(k=0) - \Delta_{\text{gap}}/2$  and  $e_3 = E_1(k=k_F) - E_2(k=k_F)$  for the electron side [18], with  $\Delta_{\text{gap}}$  defined as the gap at  $k = 0$ . For zero values of  $\Delta'$  and  $v_4$ ,  $e_2$  and  $e_3$  transitions are identical on the electron and hole sides. The finite values of  $\Delta'$  and  $v_4$  induce a significant inequality between  $e_2$  and  $e_3$  on the electron and hole sides. We first focus on the low voltage regime, where  $\omega_{\text{peak}} = e_2 = e_3$ . Because  $v_F$  and  $v_4$  always enter the Hamiltonian in the form of  $v_F k$  and  $v_4 k$  products [17], these terms give vanishing contributions at low  $V$ , where  $k$  goes to zero. Consequently,  $\omega_{\text{peak}}$  value at low bias is solely determined by  $\gamma_1$  and  $\Delta'$ , with  $\omega_{\text{peak}} = \gamma_1 + \Delta'$  and  $\omega_{\text{peak}} = \gamma_1 - \Delta'$  for the electron and hole sides, respectively. At  $V_{CN}$  (0 V), interband transitions between the two conduction bands and the two valence bands are both allowed, which leads to a broad peak centered between  $\gamma_1 + \Delta'$  and  $\gamma_1 - \Delta'$  [Fig. 3(b)]. From the two distinct low voltage  $\omega_{\text{peak}}$  values on the electron and hole sides shown in Fig. 3(b), the values of  $\gamma_1$  and  $\Delta'$  can be determined with great accuracy:  $\gamma_1 = 404 \pm 10 \text{ meV}$  and  $\Delta' = 18 \pm 2 \text{ meV}$ . Therefore, the  $\sigma_1(\omega, V)$  data at low biases clearly indicate an asymmetry between valence and conduction bands in bilayer graphene due to finite energy difference of  $A$  and  $B$  sublattices.

In order to explore the  $V$  dependence of  $\omega_{\text{peak}}$ , we plot the  $e_2$  and  $e_3$  transition energies [18] as a function of  $V$  [Fig. 3(b)], using the gap formula  $\Delta_{\text{gap}}(V)$  in [7,22] and our calculated asymmetric dispersion  $E_i(k)$  ( $i = 1, 2, 3, 4$ ) [23], with  $v_F = 1.1 \times 10^6$  m/s,  $\gamma_1 = 404$  meV,  $\Delta' = 18$  meV, and for both  $\nu_4 = 0$  and  $\nu_4 = 0.04$ . We find that  $e_2$  does not depend on  $\nu_4$  [22], whereas  $e_3$  is strongly affected by  $\nu_4$ . With a finite value of  $\nu_4$  ( $\approx 0.04$ ), an assignment of  $\omega_{\text{peak}}$  to  $(e_2 + e_3)/2$  appears to fit our data well on both electron and hole sides. The finite value of the  $\nu_4$  parameter [10] is essential to qualitatively account for the voltage dependence of  $\omega_{\text{peak}}$ , because with  $\nu_4 \approx 0$ ,  $\omega_{\text{peak}}$  follows  $e_2$  and  $e_3$  on the electron and hole sides [Fig. 3(b)], respectively, eluding a consistent description. Recently, a systematic theoretical analysis of the  $V$  dependence of  $\omega_{\text{peak}}$  and the line shape of the conductivity spectra has been reported in Ref. [20]. It is found that the infrared data presented here are consistent with a  $\nu_4$  value of  $\approx 0.05$  [20].

We stress that  $\gamma_1$  and  $\Delta'$  are determined from the low bias (low  $k_F$ ) data. Therefore the values of  $\gamma_1$  and  $\Delta'$  reported here do not suffer from the currently incomplete understanding of the infrared data at high biases [20]. The  $\gamma_1$  value ( $404 \pm 10$  meV) is directly determined from measurements of transitions between the two conduction bands or valence bands [24]. This value is more accurate than previous indirect measurements of  $\gamma_1$  [4,10,11]. The accurate determination of  $\gamma_1$  is paramount since it governs the fundamental properties of bilayer such as the quantitative behavior of the tunable band gap [4,7]. The  $\Delta'$  in bilayer graphene extracted from our data (18 meV) is about half of the value in graphite [20,21], which can be explained within the tight binding model [20].

The asymmetry between valence and conduction bands uncovered by our study has broad implications on the fundamental understanding of bilayer graphene. An electron-hole asymmetry was observed in the cyclotron resonance [8] and cyclotron mass experiments [4] in bilayer; both experiments have eluded a complete understanding so far. Our accurate determination of finite values of  $\Delta'$  and  $\nu_4$  calls for explicit account of the asymmetric band structure in the interpretation of the cyclotron data. Moreover, the different  $\Delta'$  values in bilayer graphene and graphite reveal the importance of interlayer coupling in defining the electronic properties and band structure of graphitic systems.

We thank L. M. Zhang and M. M. Fogler for their discussions on the interpretations of our data, and A. H. Castro Neto for valuable comments on the manuscript. Work at UCSD is supported by the U.S. DOE (No. DE-FG03-00ER45799). Research at Columbia University is supported by the U.S. DOE (No. DE-AIO2-04ER46133 and No. DE-FG02-05ER46215), NSF (No. DMR-03-52738 and No. CHE-0117752), NYSTAR, the Keck Foundation, and Microsoft, Project Q. The Advanced Light Source is supported by the Director, Office of

Science, Office of Basic Energy Sciences, of the U.S. Department of Energy under Contract No. DE-AC02-05CH11231.

*Note added.*—During the preparation of this Letter, we became aware of another infrared study of bilayer graphene [14].

\*zhiqiang@physics.ucsd.edu

- [1] K. S. Novoselov *et al.*, Nature (London) **438**, 197 (2005); Y. Zhang *et al.*, Nature (London) **438**, 201 (2005); A. K. Geim and K. S. Novoselov, Nature Mater. **6**, 183 (2007); A. K. Geim and A. H. MacDonald, Phys. Today **60**, No. 8, 35 (2007); A. H. Castro Neto *et al.*, arXiv:0709.1163 [Rev. Mod. Phys. (to be published)].
- [2] K. S. Novoselov *et al.*, Nature Phys. **2**, 177 (2006).
- [3] J. Nilsson *et al.*, Phys. Rev. B **73**, 214418 (2006).
- [4] E. V. Castro *et al.*, Phys. Rev. Lett. **99**, 216802 (2007).
- [5] T. Ohta *et al.*, Science **313**, 951 (2006).
- [6] E. McCann and V. I. Fal'ko, Phys. Rev. Lett. **96**, 086805 (2006); F. Guinea *et al.*, Phys. Rev. B **73**, 245426 (2006); J. Nilsson *et al.*, Phys. Rev. B **76**, 165416 (2007).
- [7] E. McCann, Phys. Rev. B **74**, 161403(R) (2006).
- [8] E. Henriksen *et al.*, Phys. Rev. Lett. **100**, 087403 (2008).
- [9] S. V. Kusminskiy *et al.*, arXiv:0805.0305.
- [10] L. M. Malard *et al.*, Phys. Rev. B **76**, 201401 (2007).
- [11] J. Yan *et al.*, Phys. Rev. Lett. **101**, 136804 (2008).
- [12] Z. Q. Li *et al.*, Nature Phys. **4**, 532 (2008).
- [13] F. Wang *et al.*, Science **320**, 206 (2008).
- [14] A. B. Kuzmenko *et al.*, arXiv:0810.2400.
- [15] Z. Q. Li *et al.*, Phys. Rev. Lett. **99**, 016403 (2007).
- [16] J. Nilsson *et al.*, Phys. Rev. Lett. **97**, 266801 (2006); D. S. L. Abergel *et al.*, Phys. Rev. B **75**, 155430 (2007).
- [17] J. Nilsson *et al.*, Phys. Rev. B **78**, 045405 (2008).
- [18] E. J. Nicol *et al.*, Phys. Rev. B **77**, 155409 (2008).
- [19] R. R. Nair *et al.*, Science **320**, 1308 (2008).
- [20] L. M. Zhang *et al.*, Phys. Rev. B **78**, 235408 (2008).
- [21] N. B. Brandt, S. M. Chudinov, and Ya. G. Ponomarev, *Semimetals 1: Graphite and Its Compounds* (North-Holland, Amsterdam, 1988).
- [22] The gap formula  $\Delta_{\text{gap}}(V)$  in [7] did not consider  $\Delta'$  and  $\nu_4$ . However, we find that finite  $\Delta'$  and  $\nu_4$  values have negligible effect on  $\Delta_{\text{gap}}$ . Specifically,  $\Delta'$  primarily modifies the  $E_1$  and  $E_4$  bands, while leaving unchanged the gap  $\Delta_{\text{gap}}$  between the  $E_2$  and  $E_3$  bands at  $k = 0$  [Fig. 2(a)]. In addition,  $\nu_4$  always appears in a term  $\nu_4 k$  in the Hamiltonian [17]; therefore, it has no effect on  $\Delta_{\text{gap}}$ .
- [23] When calculating the bands  $E_i(k)$  ( $i = 1, 2, 3, 4$ ), we assumed  $\Delta_{\text{gap}} = 0$ , which can be justified for estimating  $e_2$  and  $e_3$ .  $\Delta_{\text{gap}}$  is very small ( $< 80$  meV) under the voltages studied here [7], and hardly affects the high energy bands  $E_1(k = 0)$  or  $E_4(k = 0)$  and therefore the value of  $e_2$ . Note that a finite  $\Delta_{\text{gap}}$  is still used in the expression of  $e_2$ . Moreover,  $E_2$  and  $E_3$  bands are modified by the gap mostly at energies below  $\Delta_{\text{gap}}/2$ . Because  $E_F$  is much larger than  $\Delta_{\text{gap}}/2$  [7],  $E_2(k = k_F)$  and  $E_3(k = k_F)$  are not affected by  $\Delta_{\text{gap}}$ . Therefore, a finite gap does not modify the value of  $e_3$  compared to that with  $\Delta_{\text{gap}} = 0$ .
- [24] The uncertainty mainly stems from the shifting of the interband transition peak due to disorder effects [17,20].